

Field-Induced Phase Transitions of Repulsive Spin-1 Bosons in Optical Lattices

K. Rodríguez,¹ A. Argüelles,¹ A. K. Kolezhuk,^{2,3} L. Santos,¹ and T. Vekua¹

¹*Institut für Theoretische Physik, Leibniz Universität Hannover, Appelstrasse 2 D-30167, Hannover, Germany*

²*Institute of Magnetism, National Academy of Sciences and Ministry of Education, 36-b Vernadskii Avenue, 03142 Kiev, Ukraine*

³*Institute of High Technologies, T. G. Shevchenko Kiev National University, 64 Volodymyrska Street, 01601 Kiev, Ukraine*

(Received 21 September 2010; revised manuscript received 20 December 2010; published 9 March 2011)

We study the phase diagram of repulsively interacting spin-1 bosons in optical lattices at unit filling, showing that an externally induced quadratic Zeeman effect may lead to a rich physics characterized by various phases and phase transitions. We find that the main properties of the system may be described by an effective field model, which provides the precise location of the phase boundaries for any dimension, in excellent agreement with our numerical calculations for one-dimensional (1D) systems. Thus, our work provides a quantitative guide for the experimental analysis of various types of field-induced quantum phase transitions in spin-1 lattice bosons. These transitions, which are precluded in spin- $\frac{1}{2}$ systems, may be realized by using an externally modified quadratic Zeeman coupling, similar to recent experiments with spinor condensates in the continuum.

DOI: 10.1103/PhysRevLett.106.105302

PACS numbers: 67.85.Fg, 64.70.Tg, 67.85.Bc

Ultracold atoms in optical lattices constitute a highly controllable scenario for the analysis of strongly correlated systems, as highlighted by the realization of bosonic and fermionic Mott insulators (MIs) [1–3]. Ongoing experiments [4,5] are approaching the regime at which magnetic properties, including the long-pursued Néel antiferromagnet in spin- $\frac{1}{2}$ fermions, could be revealed. Optically trapped spinor gases, formed by atoms with various Zeeman substates, are particularly interesting: Their internal degrees of freedom result in a rich physics, mostly studied in the context of spinor Bose-Einstein condensates (BECs) [6–9]. Spinor gases in lattices are particularly exciting, since they provide unique possibilities for the analysis of quantum magnetism.

Spin-1 gases are the simplest spinor system beyond the two-component one. Depending on interparticle interactions [6,7] (given by the s -wave scattering lengths $a_{0,2}$ for collisions with total spin 0 and 2), spin-1 BECs present a ferromagnetic (FM) ground state (for $a_0 > a_2$, as in ^{87}Rb $F = 1$ [9]) or an antiferromagnetic (AFM) one (for $a_2 > a_0$, as in ^{23}Na [8]), also called polar. Spin-1 lattice bosons have also attracted a strong interest, especially the AFM case, for which a wealth of quantum phases have been predicted [10–18]. For AFM interactions, in 2D and 3D the MI states at odd filling are nematic [13,17,19], whereas in 1D quantum fluctuations lead to spontaneous dimerization [10–13,16,20–22]. The case $a_0 = a_2$ exhibits an enlarged SU(3) symmetry with a highly degenerate ground state [23].

Most spin-1 species are naturally close to this SU(3) point ($a_0 \approx a_2$), where small external perturbations, as Zeeman shifts, may have a large effect, reducing the system symmetry and thus favoring different phases. Since interactions preserve the magnetization \mathcal{M} , the linear Zeeman effect may be gauged out (although the phase

diagram depends on \mathcal{M} [14,18]). On the contrary, the quadratic Zeeman effect (QZE) plays a crucial role in spinor gases. Despite its importance, the role of the QZE in the quantum phases of spin-1 lattice bosons remains to a large extent unexplored, with the sole exception of a recent 3D mean-field analysis [18], where it was shown that for finite \mathcal{M} the QZE may lead to nematic-to-ferromagnetic (or partially magnetic) transitions.

This Letter discusses, for the first time to our knowledge, the complete phase diagram (Fig. 1) for MI phases (with unit filling) of spin-1 bosons in the presence of the QZE,

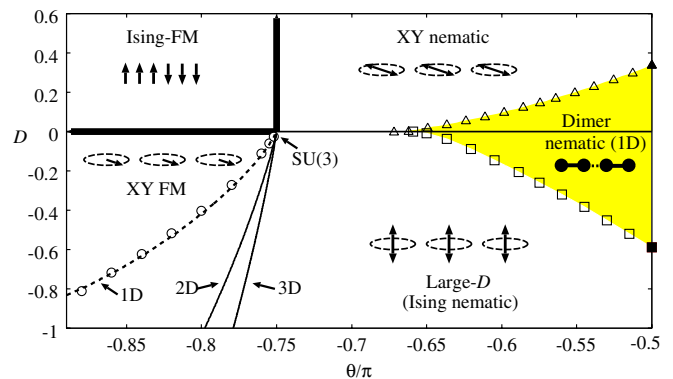


FIG. 1 (color online). Mott phases of spin-1 lattice bosons at unit filling, as a function of $\theta \equiv \arctan(J_2/J_1) - \pi$ and the QZE D together with cartoons of corresponding phases. Thick solid lines correspond to first-order phase transitions for any d . The shaded region is the dimerized phase (only in 1D), with bold (dashed) lines between the bullets indicating spontaneously enhanced (reduced) correlations between neighboring spins. Dashed ellipses visualize the XY spin planes, and single- and double-headed arrows depict spins and nematic directors, respectively. The symbols represent extrapolated 1D numerical data (see the text).

for the experimentally relevant case of a balanced mixture ($\mathcal{M} = 0$). Combining an effective field theory (for any dimension), density matrix renormalization group (DMRG) calculations, and Lanczos diagonalization, we obtain the phase boundaries, characterizing the phase transitions. We note that the QZE may be controlled by means of microwave and optical techniques [24,25]. Hence, as recently demonstrated for spinor BECs in the continuum [26], our results show that a controlled quenching of the QZE may permit the observation of field-induced phase transitions in spin-1 lattice bosons, which are precluded by simple use of the linear Zeeman effect due to conservation of \mathcal{M} and thus are absent in spin- $\frac{1}{2}$ systems. In addition, optical Feshbach resonances [27,28] permit the modification of the ratio a_2/a_0 , so that the full phase diagram discussed below may be explored with state of the art techniques.

We consider repulsively interacting ultracold spin-1 bosons in a d -dimensional hypercubic lattice, prepared in a balanced mixture ($\mathcal{M} = 0$). In free space, the interparticle interactions are characterized by the coupling constants $g_{0,2} = 4\pi\hbar^2 a_{0,2}/m_a$ (with m_a the atomic mass). In the presence of a lattice the on-site energies $\tilde{g}_{0,2}$ are proportional to $g_{0,2}$ and depend as well on lattice parameters (see, e.g., Ref. [13] for details). At integer filling, the system is in the MI regime if the (positive) on-site energies $\tilde{g}_{0,2} \gg t$, where t is the hopping amplitude between neighboring sites. In the second-order perturbation theory in t , the low-energy physics is given by superexchange processes, being described by an effective bilinear-biquadratic spin Hamiltonian [11,13]:

$$\hat{H} = -\sum_{\langle ij \rangle} [J_1 \mathbf{S}_i \cdot \mathbf{S}_j + J_2 (\mathbf{S}_i \cdot \mathbf{S}_j)^2] - DJ \sum_i (S_i^z)^2, \quad (1)$$

where \mathbf{S}_i are spin-1 operators at site i , the sum runs over nearest neighbors, $J_1 = 2t^2/\tilde{g}_2$, and $J_2 = 2t^2/3\tilde{g}_2 + 4t^2/3\tilde{g}_0$ (both are positive). The FM case ($a_0 > a_2$) corresponds to $J_1 > J_2$, whereas the AFM case ($a_2 > a_0$) results in $J_2 > J_1$. Typically, $a_0 \approx a_2$, which corresponds to the vicinity of the SU(3) point ($J_1 = J_2$). The last term in (1) describes the QZE that is characterized by the externally controllable constant $q = DJ$ and plays a crucial role in the system. In the following, we introduce the standard parameterization $J_1 = -J \cos(\theta)$, $J_2 = -J \sin(\theta)$, where θ lies in the interval $(-\pi + \arctan\frac{1}{3}, -\frac{\pi}{2})$ as the ratio g_2/g_0 varies from 0 to $+\infty$ [13], and use $J \equiv \sqrt{J_1^2 + J_2^2}$ as the energy unit ($J = 1$).

Before starting with the detailed analysis of the magnetic ground states, we provide a quick overview of the possible phases (which are sketched in Fig. 1). For $\theta < -3\pi/4$ ($J_1 > J_2$), if $D \geq 0$, the ground state is a fully polarized ferromagnet (Ising-FM), and since $\mathcal{M} = 0$ phase separation into ferromagnetic $m = \pm 1$ domains is expected. For $D < 0$ the ground state for small values of $|D|$ is an XY ferromagnet (XY FM); i.e., the system fulfills $\langle S_i^z \rangle = 0$ but presents a nonzero transversal magnetization.

This phase is ordered in dimensions $d \geq 2$, exhibiting in 1D a quasi-long-range order with leading power-law decay of XY spin correlations. For larger $|D|$ (keeping $D < 0$) there is a phase transition between the XY FM and the so-called large- D phase (also called Ising-nematic), in which all atoms are in the $m = 0$ Zeeman substate, and hence all spin correlations decay exponentially. The field-induced phase transition between large- D and XY FM is discussed in detail below.

For $\theta > -3\pi/4$ ($J_1 < J_2$) the dominant correlations are of the spin-nematic (quadrupolar) type [19,21]. A nematic phase is characterized by its nematic direction, depicted as a double-headed arrow in the sketches in Fig. 1. An XY nematic phase occurs for $D > 0$, characterized for $d \geq 2$ by $\langle (S^+)^2 \rangle \neq 0$ and $\langle \mathbf{S} \rangle = 0$, and in 1D by power-law correlations of the quadrupolar order parameter and exponentially decaying in-plane spin correlations. For $D < 0$ the large- D phase is favored. In 1D, a dimer nematic phase occurs for $D = 0$ [10–13,16,21,22]. We show below that in 1D the QZE induces a transition between the dimer phase and the XY (or Ising) nematic.

To study the phase diagram near the SU(3) point, we develop a low-energy effective field theory [29] based on spin-1 coherent states $|\psi\rangle = \sum_{a=x,y,z} (u_a + iv_a)|t_a\rangle$, where $|t_a\rangle$ are three Cartesian spin-1 states [$|t_z\rangle \equiv |m=0\rangle$, $|m=\pm 1\rangle \equiv \mp(1/\sqrt{2})(|t_x\rangle \pm i|t_y\rangle)$]. The real vectors \mathbf{u} and \mathbf{v} (defined at each lattice site) satisfy the constraints $\mathbf{u}^2 + \mathbf{v}^2 = 1$ and $\mathbf{u} \cdot \mathbf{v} = 0$. The vector \mathbf{u} plays the role of director vector for the nematic phases discussed below (double-headed arrow in the sketches in Fig. 1). The average spin on a site fulfills $\mathbf{M} \equiv \langle \psi | \mathbf{S} | \psi \rangle = 2(\mathbf{u} \times \mathbf{v})$.

The FM region $\theta < -3\pi/4$ is characterized by the magnetization length M and the Euler angles $(\vartheta, \varphi, \chi)$ which parameterize the orientation of the mutually orthogonal vector pair (\mathbf{M}, \mathbf{u}) . Assuming \mathbf{u} and \mathbf{v} to be smooth fields and performing a gradient expansion, one obtains the effective continuum field Lagrangian (see Ref. [29] for details). For $D < 0$, configurations with $\vartheta \simeq \pi/2$ and $\chi \simeq 0$ are favored. Since $(M \cos \vartheta, \varphi)$ and (M, χ) are pairs of conjugate variables, ϑ and χ become “slaves” and can be integrated out. The potential energy is minimized at $|\mathbf{M}| = M_0 = \{1 - \eta^2\}^{1/2}$, where $\eta \equiv |D|/2Z(\sin\theta - \cos\theta)$, with Z the lattice coordination number. We expand the effective action around the equilibrium value, $|\mathbf{M}| = M_0 + \delta$, integrate out δ , and obtain the effective action for φ , which can be cast in the familiar form of the $(d+1)$ -dimensional XY model:

$$\mathcal{A}_{XY} = (\Lambda^{d-1}/2g) \int d^{d+1}x (\partial_\mu \varphi)^2. \quad (2)$$

Here Λ is the ultraviolet lattice cutoff, and the coupling constant g , acting as an effective temperature, reads

$$g^{-2} = \frac{1}{2Z} \left\{ \frac{1-\eta}{\eta} + \frac{\langle \delta^2 \rangle}{2\eta^4} \right\} (1-\eta)(\lambda+1+\eta) + \langle \delta^2 \rangle \left[1 + \frac{\lambda}{2\eta^3} \right], \quad (3)$$

where $\langle \delta^2 \rangle = g_\delta C_d \pi^{1-d} \int_0^\pi dk k^{d-1} / \sqrt{m_\delta^2 + k^2}$ is the fluctuation strength and $g_\delta^2 = (8Z\eta^4)/(\lambda + 2\eta^2)$ and $m_\delta^2 = Z(1 - \eta^2)/(\lambda/2 + \eta^2)$, respectively, the coupling constant and mass of the δ fluctuations, $\lambda \equiv \tan\theta/(1 - \tan\theta)$, and $C_d^{-1} = (4\pi)^{d/2}\Gamma(d/2)$.

Model (2) describes a phase transition between XY FM and large- D occurring at a nonuniversal $g = g_c$. For $d = 1$ this is a Kosterlitz-Thouless (KT) transition, and the XY FM phase has only a quasi-long-range order. For $d \geq 2$, the phase transition belongs to the $(d + 1)$ -dimensional XY universality class, the XY FM phase is ordered with a spontaneously broken U(1) symmetry ($\varphi = \varphi_0$), and the order parameter $\langle \cos\varphi_0 S^x + \sin\varphi_0 S^y \rangle \neq 0$. Once g_c is known, Eq. (3) constitutes an implicit equation to determine the transition boundary $D(\theta)$; it has an *universal slope* for $\lambda \rightarrow \infty$ [SU(3) point] given by $\eta = 1 - O(\lambda^{-1/2})$.

We have numerically evaluated the large- D to XY FM boundary in 1D by means of DMRG calculations (following the method of Ref. [30] for up to 42 sites). We found that the most efficient way to locate the phase boundary is to study the fidelity susceptibility [31], $\chi(D) = -2\lim_{\Delta D \rightarrow 0} \ln\{|\langle \psi(D) | \psi(D + \Delta D) \rangle|^2\} / \Delta D^2$, where the quantity under the logarithm is the fidelity, i.e., the Hilbert-space distance between the ground states at two values of the QZE coupling. Figure 2(a) shows the evolution of the peak in $\chi(D)$ with increasing system size. The finite-size scaling of the peak position as a function of the number L of sites very accurately follows a $1/L^2$ law, confirming its KT character. Extrapolating the peak position to $L = \infty$ yields the curve shown in Fig. 1, which agrees perfectly with our field-theoretical description after fitting the single parameter g_c . An excellent agreement with the numerics is obtained for $g_c \approx 0.6$.

For $d \geq 2$, g_c may be estimated by neglecting fluctuations of \mathbf{M} and demanding the critical $|D|$ to match the Ising value ZJ_1 at $J_2 = 0$, yielding $g_c = (8Z/5)^{1/2}$. For a square lattice the resulting $g_c \approx 2.53$ compares favorably with the Monte Carlo result $g_c \approx 2.20$ for the classical 3D XY transition on a cubic lattice [32]. The corresponding 2D and 3D transition curves obtained from Eq. (3) are also shown in Fig. 1. For $F = 1$ ^{87}Rb in a 3D lattice of 426 nm spacing and depth of 14 recoils ($t/\tilde{g}_{0,2} \approx 0.02$, well in MI),

the large- D to XY FM transition occurs at ~ 30 mG. For 1D lattices with a transversal confinement of 12 kHz, and depth of 7 recoils ($t/\tilde{g}_{0,2} \approx 0.18$, well in MI), we expect the transition at ~ 160 mG.

For the AFM case, the effective theory can be formulated by using the de Gennes tensor $Q^{ab} \equiv u_a u_b - \delta_{ab}/3$ [33]:

$$\mathcal{A}_n = (\Lambda^{d-1}/4g_n) \int d^{d+1}x \{(\partial_\mu Q^{ab})^2 + 2\Lambda^2 m_n^2 Q^{zz}\}, \quad (4)$$

where the coupling $g_n = \sqrt{Z/2\lambda}$ vanishes at the SU(3) point [29] and $m_n^2 = D/\sin\theta$ is the QZE-induced mass. The \mathbf{u} anisotropy (see the sketch in Fig. 1) is of the easy-plane (easy-axis) type for $D > 0$ ($D < 0$). For $d \geq 2$ there is a long-range nematic order for any D , with a single transition at $D = 0$, between a gapless XY nematic with $\langle (S^+)^2 \rangle \neq 0$ at $D > 0$ and a gapped Ising nematic $\langle (S^z)^2 \rangle = 0$ at $D < 0$.

For 1D, at $D = 0$ the AFM phase presents exponentially decaying nematic (quadrupolar) correlations [albeit with a very large correlation length $\xi_n \propto e^{4\pi/g_n}$ and a tiny excitation gap $\Delta_n \propto \xi_n^{-1}$ close to the SU(3) point [20,21]]. In this phase the lowest excitations have total spin $S = 2$, which can be understood by noticing that in model (4) the magnetization \mathbf{M} is a composite field, $M_a \propto \epsilon_{abc} Q^{bd} \partial_\tau Q^{cd}$, and thus $S = 1$ excitations (which are created by spin operators) have a twice larger gap $\Delta_S = 2\Delta_n$.

However, this disordered-nematic phase [20,21] acquires a very weak long-range dimer order $\langle S_i \cdot S_{i+1} \rangle \neq \langle S_i \cdot S_{i-1} \rangle$ all the way to the SU(3) point, due to the condensation of Z_2 disclinations [12,34]. Although model (4) does not capture dimerization, it may be used to determine the boundaries of XY nematic and Ising nematic phases at small $|D|$, provided that Z_2 disclinations do not play role at the corresponding phase transitions.

For $D > 0$, the transition is KT (albeit driven by half-quantum vortices [35]), whereas at $D < 0$ the transition is Ising-like. Transition lines close to the SU(3) point fulfill $D_c^\pm \approx \pm J_2 \exp\{-4\pi/\sqrt{1 - J_1/J_2}\}$. As shown below, this analysis provides a good insight on the dimer-to-nematic transitions.

To characterize numerically the boundaries of the dimerized phase (where fidelity susceptibility remains featureless), we employed level spectroscopy analysis [36]. In a finite chain, two dimerized ground states (degenerate in the thermodynamic limit) split in energy, so the lowest excited state in the dimerized phase is unique and belongs to the $\mathcal{M} = 0$ sector. In contrast, both in the large- D phase ($D < D_c^-$) and in the XY nematic ($D > D_c^+$), the lowest excited states are twofold degenerate, having $\mathcal{M} = \pm 1$ and ± 2 , respectively. Thus, in finite chains a level crossing between the lowest excited singlet and doublet states occurs when changing D . Our extrapolated results for D_c^\pm , obtained by Lanczos diagonalization for periodic systems of up to $L = 16$ sites, are shown in Fig. 1 with $\Delta \rightarrow D_c^+$, $\square \rightarrow D_c^-$. Note that when approaching the SU(3) point our numerics cannot recover the exponentially small dimer

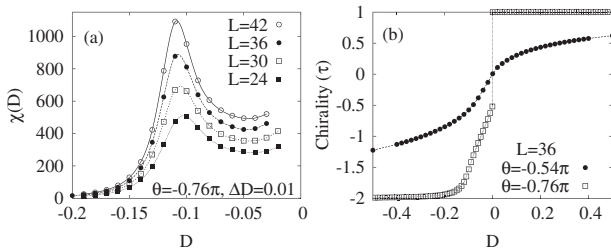


FIG. 2. (a) Evolution of the fidelity susceptibility $\chi(D)$ at the boundary between XY FM and large- D phases, with increasing system size L ; (b) chirality τ as a function of D , for two cuts at the FM ($\theta = -0.76\pi$) and nematic ($\theta = -0.54\pi$) sides.

region, which basically reduces to the $D = 0$ line. The finite-size extrapolation of D_c^+ follows a $1/L^2$ law, confirming its KT nature.

To determine the universality class of the $D = D_c^-$ transition, we have computed the central charge at $D = 0$, $\theta = -0.73\pi$ [37]. The block entanglement entropy for an open 1D system of size L , divided into two pieces of size l (block) and $L - l$ (environment), behaves as $\mathcal{S} = \frac{c}{6} \log[\frac{L}{\pi} \sin(\frac{\pi l}{L})] + A$, where c is the central charge and A is a nonuniversal constant [38,39]. Setting $l = \frac{L}{2}$, following Ref. [40], and using DMRG to evaluate \mathcal{S} for several L values, we obtain $c \approx 1.5$. The $D = D_c^+$ KT line has $c = 1$; subtracting its contribution, we get $c = \frac{1}{2}$ for the $D = D_c^-$ line, confirming its Ising nature.

Finally, we discuss the behavior of the chirality $\tau = \frac{1}{L} \sum_i (\hat{n}_{i+1} + \hat{n}_{i-1} - 2\hat{n}_{i,0}) = \frac{1}{L} \sum_i \{3(S_i^z)^2 - 2\}$, which can be easily monitored in Stern-Gerlach-like time-of-flight experiments. Figure 2(b) shows τ as a function of D . At the FM side, τ is discontinuous at $D = 0$ indicating the first-order character of the transition, which is clear since for the Ising-FM phase ($D > 0$) $\tau = 1$, while in the XY FM phase ($D < 0$) for $D \rightarrow -0$ the ground state energy is minimized at $(M, \vartheta, \chi) = (1, \frac{\pi}{2}, 0)$, and thus for $\langle (S^z)^2 \rangle \rightarrow \frac{1}{2}$ and $\tau \rightarrow -\frac{1}{2}$. At the XY FM to large- D transition, τ practically saturates to -2 for a value of D close to that obtained from the fidelity susceptibility analysis. On the AFM side the limit $D \rightarrow 0$ is nonsingular, and thus $\tau = 0$ there. The nematic-to-dimer transitions do not present any pronounced feature of τ . These transitions could be revealed experimentally by Faraday rotation techniques [41] or those recently explored in Ref. [42].

In summary, we have obtained the complete phase diagram (for any dimension) for spin-1 lattice bosons in the MI phase (at unit filling) in the presence of quadratic Zeeman coupling. Our results provide hence a quantitative guide for the analysis of field-induced quantum phase transitions in lattice bosons, which, similar to recent experiments with spinor BECs in the continuum [26], may be realized by modifying the QZE by means of microwave dressing. Starting in the large- D phase, and dynamically modifying the QZE across the transitions discussed in this Letter, should result in the FM regime in the appearance of XY FM domains, similar to those observed in spin-1 BECs [26], whereas quenches in the AFM regime should lead to nematic domains with different $\langle S_{x,y}^2 \rangle$ but homogeneous $\langle S \rangle = 0$. We stress that such field-induced transitions are precluded for spin- $\frac{1}{2}$, constituting an interesting novel feature of lattice spinor gases.

We thank A. Honecker for useful discussions. A. K. K. acknowledges the hospitality of the Institute of Theoretical Physics at the Leibniz University of Hannover and support by Grant No. 220-10 from the Ukrainian Academy of Sciences. This work has been supported by the Center for Quantum Engineering and Space-Time Research (QUEST) and the SCOPES Grant No. IZ73Z0-128058.

- [1] M. Greiner *et al.*, *Nature (London)* **415**, 39 (2002).
- [2] R. Jördens *et al.*, *Nature (London)* **455**, 204 (2008).
- [3] U. Schneider *et al.*, *Science* **322**, 1520 (2008).
- [4] R. Jördens *et al.*, *Phys. Rev. Lett.* **104**, 180401 (2010).
- [5] P. Medley *et al.*, arXiv:1006.4674.
- [6] T.-L. Ho, *Phys. Rev. Lett.* **81**, 742 (1998).
- [7] T. Ohmi and K. Machida, *J. Phys. Soc. Jpn.* **67**, 1822 (1998).
- [8] J. Stenger *et al.*, *Nature (London)* **396**, 345 (1998).
- [9] M. D. Barrett, J. A. Sauer, and M. S. Chapman, *Phys. Rev. Lett.* **87**, 010404 (2001).
- [10] E. Demler and F. Zhou, *Phys. Rev. Lett.* **88**, 163001 (2002).
- [11] S. K. Yip, *Phys. Rev. Lett.* **90**, 250402 (2003).
- [12] F. Zhou and M. Snoek, *Ann. Phys. (N.Y.)* **308**, 692 (2003).
- [13] A. Imambekov, M. Lukin, and E. Demler, *Phys. Rev. A* **68**, 063602 (2003).
- [14] A. Imambekov, M. Lukin, and E. Demler, *Phys. Rev. Lett.* **93**, 120405 (2004).
- [15] M. Snoek and F. Zhou, *Phys. Rev. B* **69**, 094410 (2004).
- [16] M. Rizzi *et al.*, *Phys. Rev. Lett.* **95**, 240404 (2005).
- [17] K. Harada, N. Kawashima, and M. Troyer, *J. Phys. Soc. Jpn.* **76**, 013703 (2007).
- [18] M.-C. Chung and S. Yip, *Phys. Rev. A* **80**, 053615 (2009).
- [19] N. Papanicolaou, *Nucl. Phys.* **B305**, 367 (1988).
- [20] A. V. Chubukov, *J. Phys. Condens. Matter* **2**, 1593 (1990).
- [21] A. V. Chubukov, *Phys. Rev. B* **43**, 3337 (1991).
- [22] G. Fáth and J. Sólyom, *Phys. Rev. B* **51**, 3620 (1995).
- [23] C. D. Batista, G. Ortiz, and J. E. Gubernatis, *Phys. Rev. B* **65**, 180402(R) (2002).
- [24] F. Gerbier *et al.*, *Phys. Rev. A* **73**, 041602(R) (2006).
- [25] L. Santos *et al.*, *Phys. Rev. A* **75**, 053606 (2007).
- [26] L. E. Sadler *et al.*, *Nature (London)* **443**, 312 (2006).
- [27] P. O. Fedichev *et al.*, *Phys. Rev. Lett.* **77**, 2913 (1996).
- [28] D. J. Papoular, G. V. Shlyapnikov, and J. Dalibard, *Phys. Rev. A* **81**, 041603(R) (2010).
- [29] B. A. Ivanov and A. K. Kolezhuk, *Phys. Rev. B* **68**, 052401 (2003).
- [30] F. Verstraete, J. J. Garcia-Ripoll, and J. I. Cirac, *Phys. Rev. Lett.* **93**, 207204 (2004).
- [31] W.-L. You, Y.-W. Li, and S.-J. Gu, *Phys. Rev. E* **76**, 022101 (2007).
- [32] A. P. Gottlob and M. Hasenbusch, *Physica (Amsterdam)* **201A**, 593 (1993).
- [33] P.-G. de Gennes and J. Prost, *The Physics of Liquid Crystals* (Oxford University, New York, 1995).
- [34] T. Grover and T. Senthil, *Phys. Rev. Lett.* **98**, 247202 (2007).
- [35] S. Mukerjee, C. Xu, and J. E. Moore, *Phys. Rev. Lett.* **97**, 120406 (2006).
- [36] K. Okamoto and K. Nomura, *Phys. Lett. A* **169**, 433 (1992).
- [37] Strictly speaking, this point is inside the dimerized phase, but since the correlation length is extremely large, the system can be considered as gapless.
- [38] V. E. Korepin, *Phys. Rev. Lett.* **92**, 096402 (2004).
- [39] P. Calabrese and J. Cardy, *J. Stat. Mech.* (2004) P06002.
- [40] L. Tagliacozzo *et al.*, *Phys. Rev. B* **78**, 024410 (2008).
- [41] K. Eckert *et al.*, *Nature Phys.* **4**, 50 (2008).
- [42] S. Trotzky *et al.*, *Phys. Rev. Lett.* **105**, 265303 (2010).